Supporting Information

Treiser et al. 10.1073/pnas.0909597107

Features	*Definition*
Angle	Reports the angle between the vertical axis and the major axis of the equivalent ellipse. Within the context of this study it would capture randomly oriented versus aligned cell populations,
Area	Reports the total actin area of each cell.
Polygonal Area	Reports the area of the polygon that defines the object's outline.
Area/Box	Reports the ratio between the area of each object and the area of the imaginary bounding box.
Aspect	Reports the ratio between the major and minor axes of the ellipse with the same area, first and second order moments of the cell.
Axis (major)	Reports the length of the major axis of the ellipse with the same area, first and second order moments of the cell.
Axis (minor)	Reports the length of the minor axis of the ellipse with the same area, first and second order moments of the cell.
Box Height	Reports the height of the smallest bounding box that completely encompasses the whole cell.
Box Width	Reports the width of the smallest bounding box that completely encompasses the whole cell.
Box Ratio	Reports the ratio between the Box Width and Box Height
Dendrites	Reports the number of 1-pixel thick open branches. Within the context of the actin cytoskeleton it represents the number of processes stemming from the cell.
Dendritic Length	Reports the total length of all dendrites.
Maximum Diameter	Reports the length of the longest line joining two outline points and passing through the centroid of the cell.
Mean Diameter	Reports the average length of the diameters.
Minimum Diameter	Reports the length of the shortest line joining two outline points and passing through the centroid of the cell.
End Points	Reports the number of 1-pixel thick processes stemming from the cell.
Maximum Feret Length	Reports the longest caliper length.
Mean Feret Length	Reports the average caliper length.
Minimum Feret Length	Reports the shortest caliper length.
Fractal Dimension	Reports the fractal dimension of the cell's outline.
Cell Area/Total Area	Reports the ratio between the area of the cell to that of the entire field of view (10x6 tile scan image).
Perimeter	Reports the length of the outline of each cell using a polygonal outline.
Perimeter2	Faster but less accurate measure of the perimeter.
Perimeter3	Reports a corrected chain code length of the cell perimeter.
Convex Perimeter	Reports the perimeter of the convex outline of each cell.
Elliptical Perimeter	Reports the perimeter of the ellipse surrounding the outline of each cell.
Perimeter Ratio	Reports the ratio of the convex perimeter to the perimeter outline of each cell
Maximum Radius	Reports the maximum distance between each cell's centroid pixel position and its perimeter.
Minimum Radius	Reports the minimum distance between each cell's centroid pixel position and its perimeter.
Radius Ratio	Reports the ratio between Max Radius and Min Radius for each object, as determined by Max Radius / Min Radius.
Roundness	Reports the roundness of each object, as determined by the following formula: (perimeter2) / (4 *π* area). Circular cells will have a roundness = 1; other shapes will have a roundness > 1.
Size (Length)	Reports the feret diameter (caliper length) along the major axis of the cell.
Size (Width)	Reports the feret diameter (caliper length) along the minor axis of the cell.
Mean Density	Reports the mean intensity of all pixels within a cell. Correlates to the average amount of fluorescently tagged phalloidin present within a given cell.
Standard Deviation of Density	Reports the standard deviation of the intensity of pixels within a cell. This represents the degree to which the phalloidin stained cytoskeleton is localized into distinct filaments of equal staining intensity.
Sum of the Density	Reports the sum of the total intensity values of all pixels within a cell. Corresponds to the total amount of positive phalloidin-staining within the cell.
Integrated Optical Density	Reports the average intensity of each object normalized by the area of the cell.
Holes	Reports the number of independent contiguous areas with no staining within a cell.
Hole Area	Reports the area of holes within an object.
Hole Ratio	Reports the ratio of the object area excluding holes, to the total area of the object, as determined by Area / (Area + Hole Area).
Margination	Reports the distribution of intensity between the center of the cell and the edge of the cell. Describes the relative spatial distribution of actin filaments within the cell.
Heterogeneity	Reports the fraction of pixels that vary more than 10% from the average intensity of the cell. Is a textural parameter that describes the degree to which the actin filaments are organized into homogenously stained structures.
Clumpiness	The fraction of heterogeneous pixels remaining in a cell after an erosion process. It reflects the object texture and the degree to which actin filaments are organized into filamentous structures.

Fig. S1. Table of 43 actin fluororeporter defined morphometric features for individual hMSCs. This table lists the 43 actin-based features quantified for each cell. The definition of the feature and its probable significance to actin filament organization are listed. Shape features are highlighted in blue, intensity features are highlighted in green, and textural/organizational features are highlighted in red.

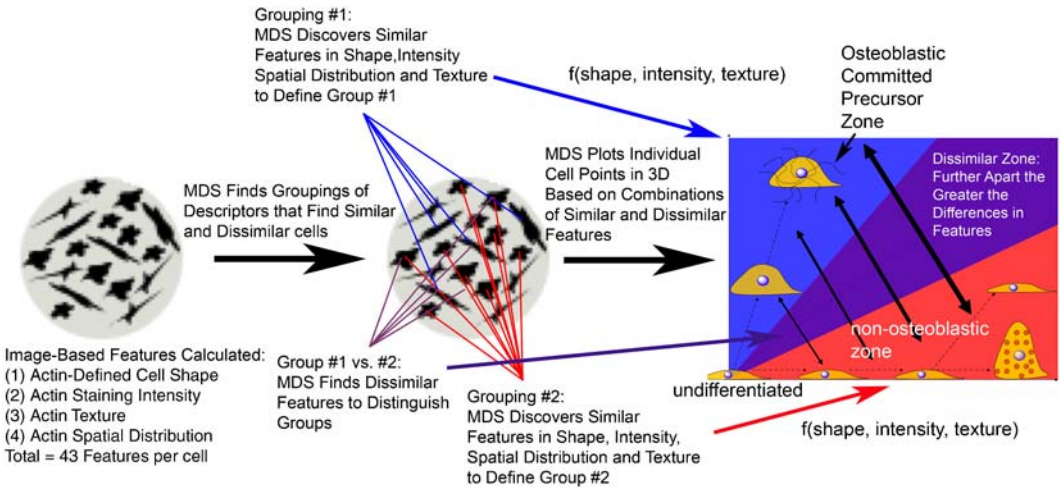

Fig. S2. Schematic of Multi-Dimensional Scaling (MDS) approach to segment cells based on actin cytoskeletal organization. A heterogeneous population of cells is cultured on a substrate, stained with fluorescently labeled phalloidin, which binds filamentous actin, and imaged at high-resolution. 43 morphometric features are calculated for each cell based on actin shape, intensity of staining, texture and spatial distribution. MDS allows the 43 features of individual cells to be grouped and remapped in 3D with their proximity to each other indicative of the similarities in their features. More similar cells are graphed closer together than less similar cells. The MDS algorithm discovers similar and dissimilar groupings of cells via a nonlinear combination of the 43 descriptors that maximizes the spatial representation of the similarities and dissimilarities between individual cells.

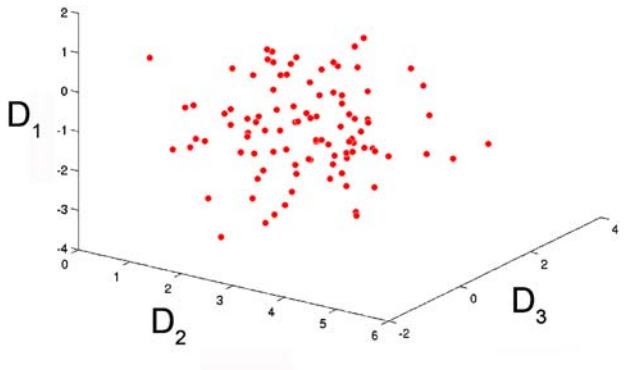

Fig. S3. Performing MDS upon a random negative control yields no clear identifiable structure. A negative control was run to confirm that the vertex-based MDS structure seen in Figs. 3–5 is not an artifact of the multidimensional scaling process itself. The synthetic negative control consisted of randomly generated values with the same mean and standard deviation as the raw data. Performing the MDS on this synthetic data set results in a graphical representation of the data lacking defined structure while maintaining its Gaussian character. There is no clear reference point or vertex from which the rest of the data deviates. Therefore the MDS clustering seen in the experimental conditions clearly results from inherent attributes of the data and is not a random effect.

Polymer	Molecular Weight (Da)	PDI	T_g (°C)	Air Water Contact Angle
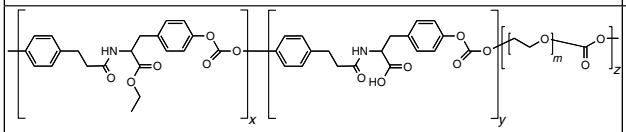 poly(82%DTE-co-10%DT-co-8%PEG $_{1K}$ carbonate)	M_n = 120K M_w = 171K	1.4	46 20	72.5°± 2.6
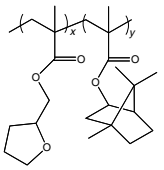 poly(71%tetrahydrofurfuryl-co-29%-isobornyl methacrylate)	M_n = 249K M_w = 514K	2.1	56	68.2°± 1.0
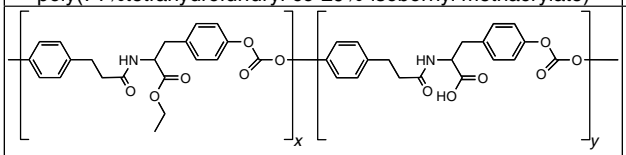 poly(90%DTE-co-10%DT carbonate)	M_n = 241K M_w = 316K	1.3	101	72.7°± 1.4
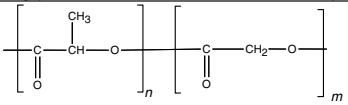 poly(50%D,L-lactic-co-50%glycolic acid)	M_n = 50K M_w = 88K	1.8	42	70.8°± 0.9
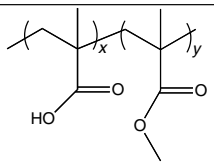 poly(70%methacrylic acid-co-30%methyl methacrylate)	M_n = 87K M_w = 107K	1.2	NF	80.1°± 1.0
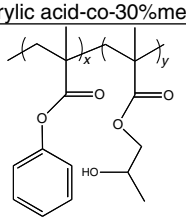 poly(78%benzyl-co-22%hydroxypropyl methacrylate)	M_n = 121K M_w = 308K	2.5	72	63.5°± 4.4
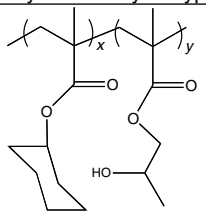 poly(30%cyclohexyl-co-70%hydroxypropyl methacrylate)	M_n = 331K M_w = 742K	2.2	92	89.9°± 2.3
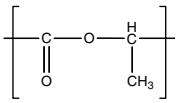 poly(L-lactic acid)	M_n = 109K M_w = 182K	1.7	66	73.7°± 0.8

Fig. S4. The single cell morphometric methodology can be used to assess hMSC differentiation on a wide array of biomaterials. The eight synthetic materials utilized to promote altered bone versus non-bone differentiation ratios are shown. Chemical formula, backbone diagram, molecular weight (M_n, M_w), polydispersity (PDI), glass transition temperatures (T_g) and air-water contact angle is reported for all the materials. All values were measured except for the T_g for PLLA and PLGA, which were obtained from the literature. As can be seen, the morphometric approach can be applied on materials representing a varied material space. Three separate classes of synthetic materials were chosen including polycarbonates, polymethacrylates, and poly(α-hydroxy ester)s.

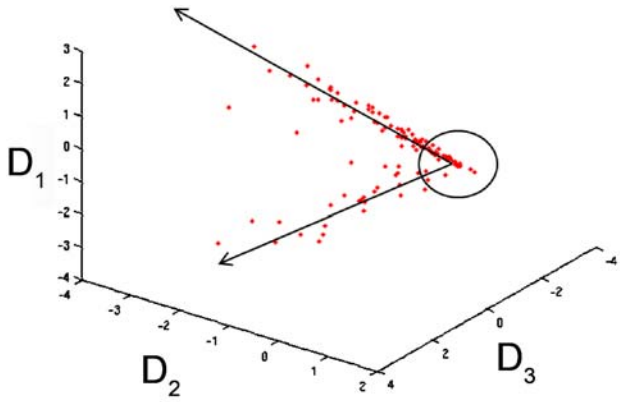

Fig. S5. hMSCs cultured on synthetic/ECM substrates demonstrate two separate definable clusters within a single image. Running of the MDS upon the individual cell morphometrics for a single sample of cells cultured upon poly(30%cyclohexyl-co-70%hydroxypropyl methacrylate) demonstrates that the MDS-processed cells are scattered via two different trajectories. It is hypothesized that these trajectories correspond to osteoblastic-committed cells and non-osteoblastic-committed cells respectively. Each point in the graph represents a single cell. All cells were taken from a single tile scan image and were cultured within the same well under a similar milieu. Cells were cultured at 21,000 cells per cm^2 in 50:50 mixed AD:OS media. These conditions were chosen to maximize the bipotential nature of the culture.

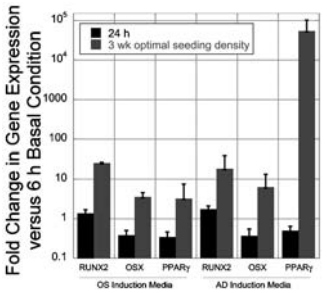

Fig. S6. hMSCs display growth factor dependent differentiation behaviors that are not detectable by gene transcription analyses within the first 24 h of culture. Polymerase chain reaction (PCR) results of mRNA transcripts of RUNX2, OSX and PPARγ for cell cultures at 24 h, and three weeks in either AD or OS induction media. For the 24 h samples cells were seeded at densities of 3,000 cells per cm^2. The three-week samples were seeded at 1,000 cells per cm^2 for OS conditions and 25,000 cells for AD conditions to promote optimal osteoblastogenesis and adipogenesis for comparisons. PCR data shown resulted from $N = 2$ independent experiments with cells from two different donors. Error bars represent the standard deviation.

24 hrs: Glass Substrates with Fibronectin Pre-treatment			Glass Substrates without Fibronectin Pre-treatment			
Donor 1 Passage 2	**Donor 2 Passage 2**	**Donor 1 Passage 4**	**24 hrs**	**48 hrs**	**72 hrs**	**96 hrs**
Perimeter2	Std. Dev. of Density	Mean Density	Fractal Dimension	Perimeter2	**All 43 Descriptors**	**All 43 descriptors**
Hole Ratio	Hole Ratio	Holes	Cell Area/Total Area	Dendrites	Mean Density	Sum of the Density
Box Height	Holes	Clumpiness	Mean Density	Cell Area/Total Area	**w/o Mean Density**	**w/o Density Sum**
Size (Width)	Size (Width)	Perimeter2	Perimeter2	Axis (Major)	Dendrites	Dendrites
Holes	Area/Box	Hole Ratio	Area	Fractal Dimension		Clumpiness
Cell Area/Total Area	Minimum Diameter	Box Width	Margination	Area/Box	**w/o Mean Density, Dendrites**	**w/o Density Sum, Dendrites, Clumpiness**
Polygonal Area	Clumpiness	Polygonal Area	Area/Box	Mean Density	Sum of the Density	Perimeter2
Box Ratio	Box Ratio	Roundness	Aspect	Minimum Diameter		Fractal Dimension
Perimeter Ratio	Mean Density	Maximum Diameter	Box Ratio	Area		Cell Area/Total Area
Fractal Dimension		Minimum Radius		Maximum Diameter		Roundness
Clumpiness		Minimum Diameter		Angle		Perimeter Ratio
Roundness		Radius Ratio			**w/o Mean Density, Dendrites, Density Sum**	
Angle					Perimeter2	
Minimum Diameter					Minimum Feret Length	
					Hole Area	
Color Designations of Morphometric Descriptors					**DT Descriptor Values in OS and AD**	
Donor-Specific	Passage-Specific	All 3 Sources			Higher OS	Higher AD

Fig. S7. A subset of cytoskeleton-based descriptors characterizes early hMSC morphological heterogeneity and indicates donor, cell passage, time, and substrate dependence. Briefly, the High content descriptor data was subjected to a complementary decision tree analysis (2-fold cross validation and 66% data splitting) to discern the most influential cytoskeletal shape, intensity, and textural descriptors underlying lineage specification for the major classification studies conducted in this study.

Descriptors appearing in the decision tree as nodes are listed in each column; each column represents different conditions: varying cell sources (donor and cell passage number) with cells seeded on fibronectin-coated glass substrates in columns 1–3 (see Fig. 3 for MDS results), and temporal evolution of descriptors from a single cell source with cells seeded on glass substrates shown in columns 4–7 (see Fig. 5 for MDS results). From cell sources Donor 1 Passage 2, Donor 2 Passage 2, and Donor 1 Passage 4 (decision tree correctly classified instances of 92%, 92%, and 86%, respectively), the descriptors in red, namely hole ratio, holes, clumpiness, and minimum diameter, appear to be important features at 24 hours (with fibronectin treatment) for identifying hMSC morphological heterogeneity between cells in OS and AD induction media regardless of cell source, indicating that these descriptors may be early morphological markers of stem cell lineage commitment. Additionally, descriptors in blue, namely perimeter2, polygonal area, and roundness, also appear to be important in identifying cellular heterogeneity in this system, but are seen to be donor-specific. Those in green, namely size (width) and box ratio, are seen to be cell passage specific. Descriptors of cells seeded on glass substrates (no fibronectin treatment) appearing in the decision trees exhibited time-dependence in showing heterogeneity in cell morphometrics in OS vs. AD induction media. Consecutive removal of descriptors appearing in the decision tree at 72 h and 96 h on glass (columns 6 and 7) show that beyond intensity based descriptors (density mean and sum), morphometric descriptors (shape and texture based descriptors) provide a reliable means of making similar comparisons (all decision trees had correctly identified instances of >80%). The results indicate that at 72 h the descriptors in purple, namely mean density, dendrites, and sum of the density, have higher values for cells in OS induction media compared with those in AD induction media. These descriptors may be used to identify early hMSC priming towards osteoblastogenesis, while higher values in hole area (shown in orange) may be used to identify adipogenesis at this time point. Descriptors shown in orange (higher values in AD induction media in comparison with OS induction media) at 96 h, namely sum of the density, clumpiness, and perimeter ratio, show that these features may be used as markers of hMSC lineage-specific priming, but their usefulness in identifying long term fates is dependent on the time point at which the descriptors were obtained.